ELSEVIER

Engineering Analysis with Boundary Elements 27 (2003) 9–21

ENGINEERING ANALYSIS *with* BOUNDARY ELEMENTS

www.elsevier.com/locate/enganabound

A hyper-singular traction boundary integral equation method for stress intensity factor computation in a finite cracked body

T. Rangelov[a,*], P. Dineva[b], D. Gross[c]

[a]*Institute of Mathematics and Informatics, Bulgarian Academy of Sciences, Sofia 1113, Bulgaria*
[b]*Institute of Mechanics, Bulgarian Academy of Sciences, Sofia 1113, Bulgaria*
[c]*Institute of Mechanics, Darmstadt University of Technology, Darmstadt 64289, Germany*

Received 20 July 2002; accepted 26 September 2002

Abstract

This paper attempts to answer the commonly raised question: what are the parameters controlling the solution accuracy and stability when the hyper-singular traction boundary-integral equations (BIEs) are used for the dynamic (time-harmonic) linear elastic fracture analysis of a finite cracked structure.

The usage of the traction BIEs together with the parabolic discretization mesh leads to hyper-singularity, when the crack lies on the boundary, even after application of a regularization procedure. In this paper two new ways, average method and shifted point method to overcome this difficulty, are proposed and compared. It is shown by numerical experiments on the examples of a cracked rectangular plate and of a cracked infinite plane that the accuracy and the convergence of the method solution depends mainly on the smoothness requirements of the solution at all collocation points.

Keywords: Hyper-singular traction boundary integral equation method; Accuracy and convergence problems; Time-harmonic stress intensity factor; Finite cracked body

1. Introduction

The BIEM is a basic technique in the numerical solutions of physics and engineering problems. However, it is well known that the conventional displacement BIE formulation degenerates for crack problems and it cannot be directly applied to crack analysis [1,2]. There are in general five methods to overcome this difficulty:

- Multidomain technique with fictitious boundaries is used in Refs. [3,4]. Here the usual displacement BIEM can be applied, but it requires more processor time.
- The usage of the Green's function for the crack problems. Here the usual displacement BIEM can be applied without crack discretization, but these functions are not available for the elastodynamic crack problems [5].
- Traction BIE, which can be obtained by differentiating the displacement representation formula, then substituting it into the Hooke's law and taking an usual limiting process. This conventional derivation of the traction BIE is based on the Betti–Rayleigh elastodynamic reciprocal theorem. The traction BIE are hyper-singular and do not converge even in the sense of Cauchy principal values (CPV) due to the additional differentiation of the stress Green's function [6]. There are two methods for the solution of these hyper-singular equations:
  - The hyper-singular integrals are regarded as Hadamard finite-part integrals and will be directly integrated analytically [7–9].
  - After regularization procedure application, the hyper-singular integrals are regularized to CPV integrals and after that the modified BIEs are solved numerically. Most regularization techniques use partial integration to shift the derivative of the stress Green's function to the unknown crack opening displacements [2,10].
- Non-hyper-singular traction BIE derivation by using a two-state conservation integral of elastodynamic [11,12].
- A combination of displacement and hyper-singular traction BIE: mixed BIEM by Chirino and Abascal [13], dual BIEM by Fidelinski et al. [14], described in the review of Chen and Hong [15], displacement and

* Corresponding author. Tel.: +359-2-979-2845; fax: +359-2-971-3649.
E-mail address: rangelov@math.bas.bg (T. Rangelov).

0955-7997/03/$ - see front matter © 2002 Elsevier Science Ltd. All rights reserved.
PII: S0955-7997(02)00107-8

traction BIDE by Sladek and Sladek [3]. These methods used parabolic discretization and semi-continuous BE to satisfy the smoothness requirements in the hyper-singular traction BIE.

From this, it is clear that the use of the displacement BIE analysis technology is limited. The complex dynamic non-symmetric crack problems for finite bodies demand the usage of the traction BIEM. This method was restricted in the past to static problems [16] or dynamic problems for crack embedded in an infinite space [17].

This paper deals mainly with the investigation of the accuracy and the convergence of the hyper-singular traction BIEM solution for time-harmonic SIF computation of finite cracked bodies.

The difference with the above-mentioned methods is that we use continuous parabolic approximation. Here some new numerical methods are proposed, named average method (AM) and shifted point method (SPM), to approximate the tangential derivatives that appear in the traction BIE. This is done in order to satisfy the smoothness requirements of the BIE solution.

The double symmetric problem of a centrally cracked rectangular plate under an uniform time-harmonic tension is chosen as a model problem where the proposed approximate schemes are validated and compared. The reasons to use this model problem in order to illustrate the accuracy problems of the solution method are

- ★ It allows comparison of both the displacement and the traction BIEM solutions due to the symmetry.
- ★ Two traction BIE formulations can be used: multi-domain technique transformed in a single region for symmetric crack problems where a quarter of the whole geometry is considered (Fig. 1b); flat crack modelling representing the displacements along the crack surface as the relative displacements between the two crack surfaces where the whole geometry is considered (Fig. 1a). These different boundary-value problems present two different situations: a crack inside a finite body and a crack lying on the internal boundary of a finite body, which is a model situation for the interface crack problems.
- ★ The chosen example is solved by Chirino and Dominguez [18], who used displacement BIEM for one quarter of the plate. Their solution will be used for a comparison with the authors' results.

The SPM numerical scheme is validated also on the test example—single line crack in a complete plane under incident time-harmonic P-wave. The test example is solved with the traction BIEM. SIF modes I and II for different angles is computed using traction formulae and is compared with the result of Chen and Sih [19].

To the authors knowledge the model problem and the test examples above are solved here for the first time using traction BIEM and continuous parabolic approximation. This is done because of the usage of the proposed new AM and SPM schemes.

The paper is organized as follows. The formulation of the elastodynamics of a two-dimensional finite cracked body by the hyper-singular traction BIE with a discussion for the solution accuracy problems is given in Section 2. The new computational AM and SPM schemes for solution of the regularized traction BIE are described also, with special emphasis on the smoothness requirements. Section 3 presents short description of the boundary-value problems solving the model problem and various numerical results are produced and interpreted, the accuracy is evaluated and recommendations are drawn down. Also a test example of

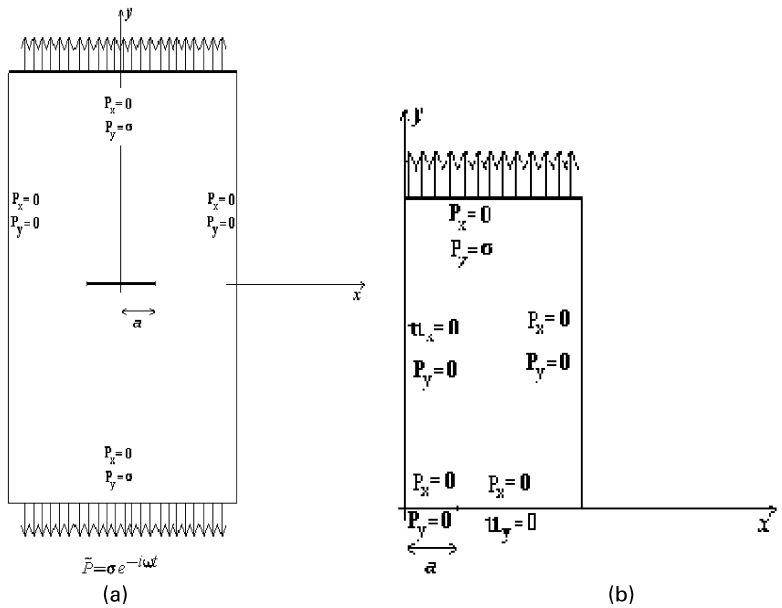

Fig. 1. (a) A centrally cracked plate. (b) One quarter of the centre-cracked plate.

a line crack in a complete plane is solved and discussed. Conclusions concerning the accuracy and the convergence problems of the hyper-singular traction BIEM for finite cracked bodies are given in Section 4.

2. Two-dimensional time-harmonic elastodynamic problem of a finite cracked body: accuracy problems of hyper-singular traction BIE

2.1. Statement of the problem

It is considered a crack in a finite body B loaded dynamically. The boundary $S = S_B \cup S_{cr}$, where $S_{cr} = S_{cr}^+ \cup S_{cr}^-$, $S_{cr}^{\pm}$ are the upper and lower faces of the crack surface, respectively, and S_B, $S_{cr}^{\pm}$ are supposed to be parts of Ljapunov surfaces. The crack surfaces are assumed to be traction free. The equations of motion of a finite two-dimensional body with homogeneous, isotropic elastic material and zero body forces in the time-harmonic elastodynamics are

$$\left(\frac{k_T^2}{k_L^2}-1\right)\left[\frac{\partial^2 u_y}{\partial x\partial y}+\frac{\partial^2 u_x}{\partial x^2}\right]+\left[\frac{\partial^2 u_x}{\partial x^2}+\frac{\partial^2 u_x}{\partial y^2}\right]+k_T^2 u_x=0$$
$$\left(\frac{k_T^2}{k_L^2}-1\right)\left[\frac{\partial^2 u_x}{\partial x\partial y}+\frac{\partial^2 u_y}{\partial y^2}\right]+\left[\frac{\partial^2 u_y}{\partial x^2}+\frac{\partial^2 u_y}{\partial y^2}\right]+k_T^2 u_y=0 \tag{1}$$

in B, where $k_T = \omega/C_T$, $k_L = \omega/C_L$ are the wave numbers, C_T, C_L are the shear and the longitudinal velocities; ω the frequency of the applied load; u_x, u_y the components of the displacement vector.

The boundary conditions prescribe traction on the part of the boundary S_p and displacements on the complementary part S_u, $S_B = S_p \cup S_u$, $S_p \cap S_u = \varnothing$.

Since the boundary-value problem is linear we can find the displacement $u_i(r,\omega)$ in the form $u_i(r,\omega) = u_i^0(r,\omega) + u_i^c(r,\omega)$ and the traction $p_i(r,\omega)$ in the form $p_i(r,\omega) = p_i^0(r,\omega) + p_i^c(r,\omega)$. Here $u_i^0(r,\omega)$, $p_i^0(r,\omega)$ are produced by the loading on S_B in the crack-free body and $u_i^c(r,\omega)$, $p_i^c(r,\omega)$ are produced in the cracked body by the load $p_i^c(\eta,\omega) = -p_i^0(\eta,\omega)$ for $\eta \in S_{cr}$ and all loads $u_i^c(r,\omega)$, $p_i^c(r,\omega)$ are zero on S_u, S_p correspondingly.

2.2. Displacement BIE and hyper-singular traction BIE formulation of the problem

Here we closely follow the BIE formulation of Sladek and Sladek [2] adapted to the two-dimensional time-harmonic case. In the crack-free case the functions $u_i^0(r,\omega)$, $p_i^0(r,\omega)$ satisfy the following set of displacement BIE:

$$c_{ij}u_j^0(r,\omega) = \int_{S_B} U_{ij}^*(r,r_0,\omega)p_j^0(r_0,\omega)\mathrm{d}S_{r_0} - \int_{S_B} P_{ij}^*(r,r_0,\omega)u_j^0(r_0,\omega)\mathrm{d}S_{r_0} \tag{2}$$

Here, c_{ij} are constants depending on the geometry at the collocation point r; r, r_0 denote the position vectors of the field and running points, respectively; U_{ij}^*, P_{ij}^* are the displacement and the traction fundamental solutions of Eq. (1) given in Appendix A.

The traction $p_i^0(\eta,\omega)$ on the imaginary crack in the 'crack-free' case can be calculated after solution of the crack-free state problem.

For the hyper-singular traction BIE with unknowns $u_i^c(r,\omega)$, $p_i^c(r,\omega)$ some integrals do not converge even in the sense of CPV, the regularization techniques of Sladek and Sladek [2] is applied. This regularization procedure uses partial integration to shift the derivatives of the traction fundamental solution to the unknown displacements and crack opening displacements. The traction BIE for the domain B after the regularization are

$$\begin{aligned} p_l^c(\xi^+,\omega) &= -p_l^0(\xi^+,\omega) \\ &= C_{lmjr}n_m(\xi^+)\Big\{-\int_{S_B} D_r U_{ij}^*(\eta-\xi^+,\omega)p_i^c(\eta,\omega)\mathrm{d}S_\eta \\ &\quad + C_{iskt}\Big[\int_{S_{cr}^+}\Delta K_{rs}^i D_t U_{kj}^*(\eta-\xi^+,\omega)\mathrm{d}S_\eta \\ &\quad + \int_{S_B} K_{rs}^i D_t U_{kj}^*(\eta-\xi^+,\omega)\mathrm{d}S_\eta\Big] \\ &\quad - \rho\omega^2\Big[\int_{S_{cr}^+}\Delta u_i^c(\eta,\omega)n_r(\eta)U_{ij}^*(\eta-\xi^+,\omega)\mathrm{d}S_\eta \\ &\quad + \int_{S_B} u_i^c n_r(\eta)U_{ij}^*(\eta-\xi^+,\omega)\mathrm{d}S_\eta\Big]\Big\} \end{aligned} \tag{3}$$

$$\begin{aligned} p_l^c(\xi^*,\omega) &= C_{lmjr}n_m(\xi^*)\Big\{-\int_{S_B} D_r U_{ij}^*(\eta-\xi^*,\omega)p_i^c(\eta,\omega)\mathrm{d}S_\eta \\ &\quad + C_{iskt}\Big[\int_{S_{cr}^+}\Delta K_{rs}^i D_t U_{kj}^*(\eta-\xi^*,\omega)\mathrm{d}S_\eta \\ &\quad + \int_{S_B} K_{rs}^i D_t U_{kj}^*(\eta-\xi^*,\omega)\mathrm{d}S_\eta\Big] \\ &\quad - \rho\omega^2\Big[\int_{S_{cr}^+}\Delta u_i^c(\eta,\omega)n_r(\eta)U_{ij}^*(\eta-\xi^*,\omega)\mathrm{d}S_\eta \\ &\quad + \int_{S_B} u_i^c n_r(\eta)U_{ij}^*(\eta-\xi^*,\omega)\mathrm{d}S_\eta\Big]\Big\} \end{aligned} \tag{4}$$

Here $C_{ijkl} = \lambda\delta_{ij}\delta_{kl} + \mu(\delta_{ik}\delta_{jl} + \delta_{il}\delta_{kj})$, $K_{rs}^i = [n_r(\eta)D_s - n_s(\eta)D_r]u_i^c(\eta,\omega)$, ρ is density, λ, μ are Lame constants, $\Delta K_{rs}^i = [n_r(\eta)D_s - n_s(\eta)D_r]\Delta u_i^c(\eta,\omega)$, $D_r = \partial/\partial\eta_r$ and ξ^+, ξ^* are field points on S_{cr}^+ and S_B, respectively. When a surface crack intersects the outer boundary, all the equations, which have been written for an internal crack in a finite body, are valid provided that $\xi^+ \in S_{cr}^+ \backslash (S_{cr}^+ \cap S_B)$, $\xi^* \in S_B \backslash (S_B \cap S_{cr}^+)$.

The unknowns in Eqs. (3) and (4) are the displacements and the tractions $u_i^0(r,\omega)$, $p_i^0(r,\omega)$, $u_i^c(r,\omega)$, $p_i^c(r,\omega)$ on S_B and the crack opening displacement $\Delta u_i^c(\eta,\omega)$ on S_{cr}^+. Eqs. (3) and (4) are boundary integro-differential equations (BIDE) and functions K_{rs}^i, ΔK_{rs}^i are the tangential derivatives

of the displacements which have to be represented by the unknowns.

The solution of the problem is a vector-valued function $u_i^c \in C^{1,\alpha}(S)$ correspondingly $p_i^c \in C^{0,\alpha}(S)$, $0 < \alpha \leq 1$, i.e. tangential derivatives $u_{i,j}^c$ on the boundary should be Hölder continuous [6], where $C^{k,\alpha}(S)$ is the set of k times differentiable functions whose kth derivatives are Hölder continuous with a constant α. Under these conditions the right hand side of the traction BIDE is well defined.

At the end of this section we would like to comment on some difficulties connected with the numerical solution of the regularized traction BIDE, applied for the solution of elastodynamics problems of finite or infinite cracked bodies. Krishnasamy et al. [20] note that the regularization process lowers the integrand singularity so that the integral of the limit exists, but this is at the expense of the tangential derivative of u_i^c, which is unbounded at the crack-edges, so the regularization process is complicated, and may not be possible, for all vector problems. The nature of the hyper-singular traction BIE leads to a special 'more singular' integral, which exists in the sense of the CPV or Hadamar finite-part integral, which fact requires smoother representation for the displacement. Martin and Rizzo [21] emphasized that the role of this smoothness requirement in the algorithms for a computation of these integrals is rich ground for research.

The authors recommend that the understanding where and why the smoothness is required will permit more stable and accurate solution. The aim of this study is to define and to show by numerical results which are the main parameters controlling the traction BIDE solution accuracy and stability.

2.3. Numerical solution of the problem by BEM

The numerical solution of the problem follows the usual procedures of the BEM. The boundary is descritized into elements using parabolic approximations of the boundary geometry, the displacement and the traction.

2.3.1. Interpolation functions

It is used a discretization of the boundary $S = S_B \cup S_{cr} = \bigcup_1^M \Gamma_s$. Denote by u_i^s, p_i^s the components of displacement and traction on the sth boundary element (BE), then $u_i^s = u_i \chi_s$, $p_i^s = p_i \chi_s$ where χ_s is the characteristic function on Γ_s, i.e.

$$\chi_s(x,y) = \begin{cases} 1, & (x,y) \in \Gamma_s \\ 0, & (x,y) \notin \Gamma_s \end{cases}$$

The next principles are used for approximation of the displacement u_i, its tangential derivatives $u_{i,j}$ and traction p_i :

(Hö) Hölder continuity. Functions $u_i \in C^{1,\alpha}(S)$, $u_{i,j} \in C^{0,\alpha}(S)$, $p_i \in C^{0,\alpha}(S)$. These conditions have to be satisfied at least at the collocation points.

(Cr) Behaviour at the crack-tips. The asymptotic expressions for the displacement and for the traction near the crack-tip in the two-dimensional case are well known [22]. The asymptotic behaviour of the displacement is $u_i \sim O(\sqrt{r})$ and of the traction is $p_i \sim O(1/\sqrt{r})$.

(Irr) Irregular points. A point at which the boundary is not smooth, correspondingly the normal vector does not exist, or the (Hö) conditions fails is defined as irregular point. The crack-tip and the corners of a cracked body are particular examples of irregular points. Since the traction BIDE exists only at the points where the interpolation functions are Hölder continuously differentiable and the boundary must be smooth, the irregular points (tips and corners) should not be used as collocation points.

2.3.2. Standard continuous quadratic approximation and its disadvantages

Three nodes and three shape functions N_k, given in Appendix C determine the quadratic element. The transformation law that is needed in passing from the global coordinate system to intrinsic coordinates is given in Appendix B. If Γ_s is an ordinary BE the approximation of u_i^s, p_i^s is

$$u_i^s(\xi) = \sum_1^3 u_i^{sk} N_k(\xi), \qquad p_i^s(\xi) = \sum_1^3 p_i^{sk} N_k(\xi) \tag{5}$$

here u_i^{sk} denotes the ith displacement component in the kth local node of the sth boundary element.

Let us now verify how the standard quadratic approximation satisfy the principles (Cr), (Hö) and (Irr).

In order to satisfy the principle (Cr) two special crack-tip boundary elements are used, following Blandford et al. [23]: a quarter-point boundary element (QP-BE) modeling the asymptotic behaviour of the displacement and a traction singular QP-BE (SQP-BE) modeling the asymptotic behaviour of the traction. The special shape functions N_k^* for the traction SQP-BE are given in Appendix C. The approximations for u_i^s, p_i^s in the case of traction SQP-BE are

$$u_i^s(\xi) = \sum_1^3 u_i^{s,k} N_k(\xi), \qquad p_i^s(\xi) = \sum_1^3 p_i^{s,k} N_k^*(\xi) \tag{6}$$

Approximations (5) and (6) are continuous at the collocation points. The tangential derivatives of the displacements at the nodal points are expressed as derivatives of the approximated displacements.

$$\frac{\partial}{\partial r_j}(u_i^s) = \frac{\partial u_i^s}{\partial \xi}\frac{\partial \xi}{\partial r_j} = \sum_1^3 u_i^{sk}\frac{\partial N_k(\xi)}{\partial \xi}\frac{\partial \xi}{\partial r_j} = \sum_1^3 u_i^{s,k} N_k' \frac{\partial \xi}{\partial r_j}$$

$$= \sum_1^3 u_i^{s,k} N_k' \xi_{,j} \tag{7}$$

here: $k = 1, 2, 3$, $i = x, y$, $j = x, y$; $N_k'(\xi)$ are given in Appendix C.

When the collocation point does not coincide with the initial or the final point of the boundary element, then the principle (Hö) is satisfied.

We shall name below the initial or the final node on the BE also as odd node or odd point since when we are numbering all nodes in a subsequent order the initial or the final node appear with an odd number.

It is evident from Eq. (7) that the approximation of the tangential derivatives of the displacement does not satisfy (Hö) at the odd points of the BE, since $N'_3(1) = \frac{3}{2} \neq N'_1(-1) = -\frac{3}{2}$. It is a common practice to have the collocation points on the nodes of the element where solution is continuous, but does not satisfy the smoothness requirement. To circumvent this problem, one could choose non-conforming elements, where the collocation points are away from the nodes. If the collocation points are located at the nodes of the element, spurious results would be obtained [18]. Such results seem to change dramatically with changes in the discretization mesh.

At the corners the boundary is not smooth and the normal vector does not exist. At the crack-tips the (Hö) condition fails. So, the irregular points should not be used as collocation points [6].

At the end we would like to summarize that the standard continuous quadratic approximation can be used only after overcoming the following disadvantages: the irregular points of a finite cracked body, i.e. crack-tips, corners and the odd discretization nodes should not be used as collocation points in the traction BIEM because the traction BIDE is not well defined in these points and this will lead to computational errors. In order to use the standard parabolic approximation avoiding the above-mentioned obstacles we need to choose an appropriate parabolic approximation for u_i, p_i, $u_{i,j}$ near the irregular point and near the odd collocation points such that the principle (Hö) to be fulfilled. We propose below two different ways for this aim.

2.3.3. Computational schemes for overcoming the disadvantages of the standard continuous quadratic approximation

Numerical scheme AM. This approximation method helps in overcoming the disadvantage of the quadratic approximation at the odd discretization nodes.

The next approximation is proposed for the tangential derivatives of the displacement on the BE Γ^s with three local nodes z_k^s, $k = 1, 2, 3$:

$$u_{i,j}^s(\xi) = \sum_1^3 v_i^{s,k} N_k \xi_{,j} \tag{8}$$

where $v_i^{s,k}$ is the average value of the tangential derivatives of u_i^s over elements Γ^{s-1}, Γ^s, Γ^{s+1} at z_k^s ($k = 1$ or 3). Note that in this case $v_i^{s-1,3} = v_i^{s,1}$ and the condition (Hö) is fulfilled. This scheme gives a global approximation of $u_{i,j}^s$—on each odd collocation point we get the average value of $u_{i,j}^s$ over the elements Γ^{s-1}, Γ^s, Γ^{s+1}.

The $v_i^{s,k}$-value is given by

$$\begin{pmatrix} v_i^{s,1} \\ v_i^{s,2} \\ v_i^{s,3} \end{pmatrix} = \begin{pmatrix} \frac{1}{2l'_{s-1}} & -\frac{2}{l'_{s-1}} & \left(\frac{3}{2l'_{s-1}} - \frac{3}{2l'_s}\right) & \frac{2}{l'_s} & -\frac{1}{2l'_s} & 0 & 0 \\ 0 & 0 & -\frac{1}{l'_s} & 0 & \frac{1}{l'_s} & 0 & 0 \\ 0 & 0 & \frac{1}{2l'_s} & -\frac{2}{l'_s} & \left(\frac{3}{2l'_s} - \frac{3}{2l'_{s+1}}\right) & \frac{2}{l'_{s+1}} & -\frac{1}{2l'_{s+1}} \end{pmatrix} \begin{pmatrix} u_i^{s-1,1} \\ u_i^{s-1,2} \\ u_i^{s,1} \\ u_i^{s,2} \\ u_i^{s+1,1} \\ u_i^{s+1,2} \\ u_i^{s+1,3} \end{pmatrix} \tag{9}$$

If Γ^{s-1}, Γ^s, Γ^{s+1} are ordinary BE, then $l'_m = l_m$—the length of the BE Γ^m. Note that the principle (Hö) is satisfied for the odd collocation points $u_i^{s-1,3} = u_i^{s,1}$, $u_i^{s,3} = u_i^{s+1,1}$.

If Γ^s is a right QP-BE just before the crack-tip, Γ^{s+1} is a left SQP-BE and Γ^{s-1} is not a crack-tip BE, then $l'_s = 2l_s$. If Γ^s is a left SQP-BE, next to the crack-tip, Γ^{s-1} is a right QP-BE, Γ^{s+1} is not a crack-tip BE, then $l'_s = 2l_s$. In all the other cases $l'_s = l_s$.

As can be seen from the traction BIDE (3) and (4) the unknowns are tractions p_i^c, displacements u_i^c, Δu_i^c and their tangential derivatives $u_{i,j}^s(\xi) = \sum_1^3 v_i^{s,k} N_k \xi_{,j}$, i.e. values $v_i^{s,k}$ become unknowns too. However, adding relation (9), the tractions and the displacements are the single unknowns in the traction BIDE.

Numerical scheme SPM. This approximation method is used to overcome the disadvantage of the quadratic approximation at the odd discretization nodes, corners and crack-tips.

A further possibility to use the standard global parabolic approximation for $u_i^s, p_i^s, u_{i,j}^s$ is to use all even nodal points as collocation points, but instead the odd nodal points to use points close to them—named shifted points. We use the possibility to express unknowns u_i^s, p_i^s at the collocation points (they are now internal points of the BE) by the unknowns at the nodes of the boundary element using their parabolic approximation over the element. This allows us to form a global algebraic system for the unknowns at the boundary nodal points.

For example, let the s-th BE Γ^s and the $s+$ -1th BE Γ^{s+1} are with nodal points z_1^s, z_2^s, z_3^s and z_1^{s+1}, z_2^{s+1}, z_3^{s+1}

correspondingly, where $z_3^s = z_1^{s+1}$. We use as a collocation point instead of the point z_1^{s+1} the point which is close to it, i.e. $z_{11}^{s+1} \in (z_1^{s+1}, z_2^{s+1})$. Suppose, for example, that the unknown on the BE Γ^s and Γ^{s+1} is p_j and under Eq. (6) it can be presented as

$$p_j(z) = \sum_1^3 p_j^{s+1,k} N_k(\xi), \qquad \text{on } \Gamma^{s+1} \tag{10}$$

where

$$\xi = 2\frac{|z - z_1^{s+1}|}{|z_3^{s+1} - z_1^{s+1}|} - 1$$

and $z = (x, y)$, $|z| = \sqrt{x^2 + y^2}$, (Appendix B).

For the unknown $p_j^{s,3} = p_j^{s+1,1}$ at the node $z_3^s = z_1^{s+1}$ we have to form one linear equation following the standard procedure of BIEM. Using the traction BIEs (3) and (4) we form an equation with a field point z_{11}^{s+1} and obtain an expression for $p_j(z_{11}^{s+1})$ through all unknowns at the nodal points, which is written in the form

$$p_j(z_{11}^{s+1}) = A^s p_j^{s,3} + A^{s+1} p_j^{s+1,1} + \Sigma \tag{11}$$

where Σ contained all the other unknowns. Coefficient A^s is calculated solving a regular integral over Γ^s, while A^{s+1} is calculated solving a CPV integral over Γ^{S+1}.

On the other side over the BE Γ^{s+1} due to the parabolic approximation (10) $p_j(z_{11}^{s+1})$ is represented as

$$p_j(z_{11}^{s+1}) = p_j^{s+1,1} N_1(\xi_{11}^{s+1}) + \sum_{k=2}^3 p_j^{s+1,k} N_k(\xi_{11}^{s+1}) \tag{12}$$

where

$$\xi_{11}^{s+1} = 2\frac{|z_{11}^{s+1} - z_1^{s+1}|}{|z_3^{s+1} - z_1^{s+1}|} - 1$$

Replacing $p_j(z_{11}^{s+1})$ from Eq. (12) into Eq. (11) we obtain the equation

$$(N_1(\xi_{11}^{s+1}) - A^s - A^{s+1}) p_j^{s+1,1} = \Sigma \tag{13}$$

Note that for a.e. z_{11}^{s+1} the coefficient of $p_j^{s+1,1}$ is not equal to zero because $N_1(\xi_{11}^{s+1})$ is real and $\mathrm{Im}(A^s + A^{s+1}) \neq 0$ due to the analyticity of the modified Bessel functions which form the time-harmonic fundamental solution and its traction (Appendix A).

For the unknowns at every odd nodal point, at every corner nodal point and at the crack-tip, in the case the crack-tip is a part of the boundary, we form equations using the shifted points as field points repeating the above described procedure. In such a way at all collocations points the principles (Hö), (Cr) and (Irr) are fulfilled.

It is a common truth that the satisfaction in the approximation of u_j and p_j of the prescribed by the theory of elliptic partial differential equations requirements for their smoothness on the boundary and for their asymptotic behaviour near the crack-tip lead to a stable and to an accurate numerical solution. The advantages of the proposed AM and SPM schemes are that they help to solve the traction BIE in the case when the continuous parabolic BE are used, i.e. the approximation of the solutions u_j, p_j is continuous. This is contrary to the application of the non-conforming BE where in order to solve properly the singular integrals, the approximation of u_j, p_j is set to be discontinuous. So, the preferences should be given to these numerical schemes where the traction BIE is solved and a priori conditions on u_j, p_j as (Hö) and (Cr) take place.

2.3.4. Evaluation of the integrals obtained after discretization

After discretization the following types of integral appear:

(i) The described above approximations of u_i, p_i lead to the integrals of the type (a) $\int_{-1}^{1} P_{ij}^*(\xi) N_k(\xi) J \, \mathrm{d}\xi$, (b) $\int_{-1}^{1} U_{ij}^*(\xi) N_k(\xi) J \, \mathrm{d}\xi$ and (c) $\int_{-1}^{1} U_{ij}^*(\xi) N_k^*(\xi) J \, \mathrm{d}\xi$ in the displacement BIE. Here J is the Jacobian given in Appendix B.

The integrals $\int_{S_B} D_r U_{ij}^*(\eta, \xi^+, \omega) p_i^c(\eta, \omega) \mathrm{d}S_\eta$ in the regularized traction BIDE (3) and (4) lead to integrals of the type (f1) $\int_{-1}^{1} U_{ij,m}^*(\xi) N_k(\xi) J \, \mathrm{d}\xi$ and (f2) $\int_{-1}^{1} U_{ij,m}^*(\xi) N_k^*(\xi) J \, \mathrm{d}\xi$ for the ordinary and for the special crack-tip SQP-BE, respectively. The integrals $\int_{S_B} u_i^c n_r(\eta) U_{ij}^*(\eta - \xi^*, \omega) \mathrm{d}S_\eta$ lead to the integrals of the type (b).

The kernels of the integrals of the type (a), (f1) and (f2) have singularities at least like $\mathrm{O}(1/(\alpha \pm \xi))$, for $\xi \to \pm\alpha$, $\alpha \in [-1, 1]$ that leads to the CPV integrals for $\alpha \neq \pm 1$. The kernels of the integrals of the type (b) and (c) have singularities at least like $\mathrm{O}(\ln(\alpha \pm \xi))$ for $\xi \to \pm\alpha$, $\alpha \in [-1, 1]$ which leads to non-singular integrals. Integrals of the type (a) for $\alpha = \pm 1$ appear only at the usage of displacement BIE. In this case we use the fact that the node point belongs to the joint BEs and by appropriate variables change the integral over the both BE is obtained and it is at least CPV integral.

(ii) The described above approximations of $u_{i,j}$ lead to the next type of integrals $\int_{S_B} K_{rs}^i D_t U_{kj}^*(\eta - \xi^+, \omega) \mathrm{d}S_\eta$, i.e. (d) $\int_{S_B} U_{kj,l}^* \sum_{s=1}^M (\chi_s u_i^s)_{,j} \, \mathrm{d}\eta$. These integrals are the sum of integrals (d1) $\int_{S_B} U_{kj,l}^* \sum_{s=1}^M \chi_s u_i^s{}_{,j} \, \mathrm{d}\eta$ and (d2) $\int_{S_B} U_{kj,l}^* \sum_{s=1}^M \chi_{s,j} u_i^s \, \mathrm{d}\eta$. When the field point is an odd point on the BE the integral (d2) is infinite. To avoid these difficulties we can use the properties of δ-function [24], the asymptotic behaviour of $U_{ij,m}^*(s)$ for $s \to 0$ and the fact that we may compare the values of (d2) over the BEs on both the sides of the given collocation point. The infinite parts of the integrals of the type (d2) vanish for all collocation points except for the crack-tips.

If the nodal point coincides with the crack-tip, the kernels of the integrals of the type (f1), (f2) and (d1), which appear only in the regularized traction BIE, have singularities like $\mathrm{O}(1/(1 \pm \xi)^2)$, for $\xi \to \pm 1$ and it is not possible to use the crack-tip as a collocation point. For this reason it is necessary to apply the SPM scheme for the unknowns on the crack-tip. We form the equation using the shifted point close

to the crack tip and the integrals are at least CPV integrals. This situation appear only in the case when the crack is part of the boundary, because for the internal crack on the crack-tip are satisfied boundary conditions and there are no unknowns.

The regular integrals are computed employing the Gaussian quadrature scheme. All singular integral and integrals with logarithmic singularity are solved analytically on the small neighbourhood of the field point, using the approximation of the fundamental solution for a small argument (Appendix B) and numerically on the other part of the BE.

After discretization of the displacement and the regularized traction BIEs, overcoming of weak and strong singularities in the obtained integrals and satisfaction of the given boundary conditions, an algebraic complex system of equations according to the unknowns is obtained and solved.

3. Test examples

3.1. Centrally cracked plate

The described AM and SPM schemes are illustrated and compared for the case of a finite cracked body. The model problem is a rectangular plate Ω^{w}, with a central crack in it, subjected to uniform time-harmonic tension $\sigma\, e^{-i\omega t}$ applied on the two opposite sides. The amplitude of the time-harmonic load is σ and ω is the frequency. The geometry of the problem is shown in Fig. 1a. The plate's boundary is Γ^{w}.

Due to the symmetry it is possible to consider the problem in a quarter domain Ω^{q} with a boundary Γ^{q} (Fig. 1b). The physical and geometrical properties of the central cracked plate are density $\rho = 0.5 \times 10^{-5}$ kg/mm^3; Lame constant $\lambda = 0.115385 \times 10^{6}$ N/mm^2, Poisson module $\nu = 0.3$, Shear module $\mu = 0.76923 \times 10^{5}$ N/mm^2, and the plate's sizes 20 mm $\times$ 40 mm. The value of the amplitude of time-harmonic load is $\sigma = 400$ N/mm^2 and the crack size is $2a = 5$ mm. The BE mesh is given in Fig. 2.

The next boundary-value problems are solved:

Q—Governing equations (1) with the boundary conditions for a quarter of the geometry using the displacement and the traction BIEM;
W—Governing equations (1) with the boundary conditions for the whole geometry using the traction BIEM.

The proposed numerical schemes overcome the disadvantages of the continuous approximation at the odd nodes, corners and crack-tips in the Q problem and in the odd nodes and corners in the W problem. Only the SPM scheme is used for the crack-tips, while for the odd nodes and for the corners are used both SPM or AM schemes.

These two boundary value problems are essential in understanding the accuracy of the numerical method applied for more complicated problems as dynamic behaviour of the multilayered finite solid with internal and interface cracks [25,26].

In this study a number of parameters (which control the accuracy and stability of the traction BIEM) are varied and

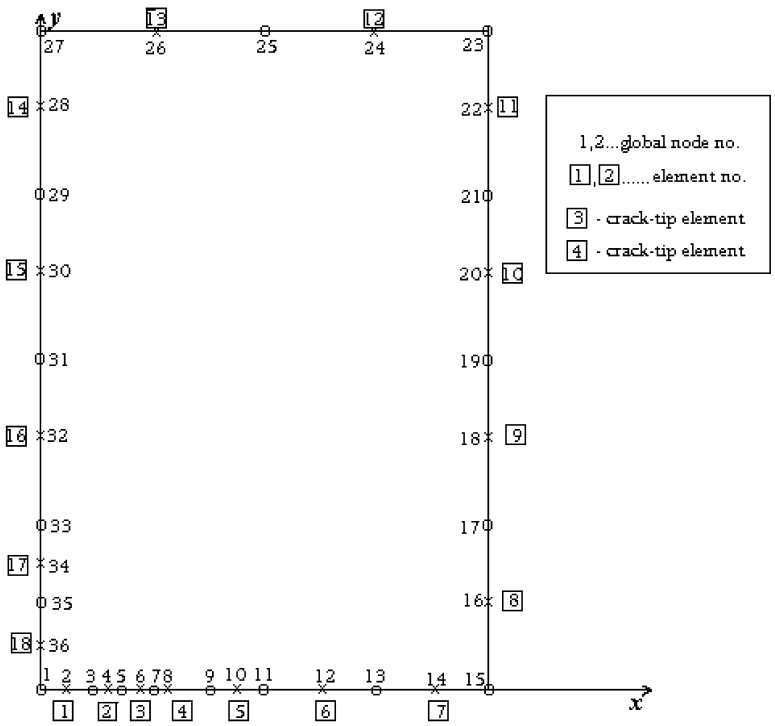

Fig. 2. The BE mesh.

their influence on SIF calculation is assessed. These parameters are the way of satisfaction of the smoothness requirements in all irregular points—corners, crack-tips and odd nodes; the frequency of the applied dynamical load; the length of the crack-tip QP-BE l_{QP} and the length of the crack-tip SQP-BE l_{SQP}.

A Fortran code is created on the base of a quadratic shape functions and numerical schemes of the AM and SPM for overcoming of the described in Section 2.3.2 disadvantages of the standard quadratic approximation. As a base for comparison it is used the result of Chirino and Dominguez [18], who solved the same test example using displacement BIEM for a quarter of the plate. The percentage error for SIF calculation is defined as:

$$\mathrm{Err} = \frac{K_{\mathrm{I}}^{\mathrm{CD}} - K_{\mathrm{I}}^{\alpha}}{K_{\mathrm{I}}^{\mathrm{CD}}}\%$$

where $K_{\mathrm{I}}^{\mathrm{CD}}$ is the result for SIF I-mode in Chirino and Dominguez [18] and K_{I}^{α}, where $\alpha = Q$, W is the authors one. SIF calculation is done by the two point displacement formulae at the crack-tip QP-BE (Appendix D).

The magnitude of the mode I dynamic SIF, normalized by $\sigma\sqrt{\pi a}$ and obtained by the traction BIE and SPM scheme for solution of the Q problem is compared with the results of Chirino and Dominguez [18]. The comparison is shown versus frequency in Fig. 3. Both the solutions are in agreement. The following crack-tip BE lengths are used $l_{QP} = 0.2a$ and $l_{SQP} = 1.255$ mm. Note that the computed SIF using the AM scheme gives the same result.

Fig. 4 investigates the parameters, which control the accuracy and the stability of the solution of the boundary-value problem W obtained by the traction BIEM. Here both schemes AM and SPM are compared for two frequencies: $k_{\mathrm{T}}a = 0.05$, $k_{\mathrm{T}}a = 0.1$. Fig. 4a and b reveals the dependence of the percentage error for SIF calculation on the ratio l_{QP}/a and the frequency of the applied dynamic load. Both proposed schemes work accurate and with a good convergence. The best accuracy for both schemes of the AM and SPM is obtained for values of l_{QP}/a close to 0.2.

Figs. 5 and 6 show how the accuracy of the traction BIE for solution of the problem Q depends on the frequency, on the discretization mesh near the crack-tip and on the way of satisfaction of the smoothness requirements in the collocation points. Fig. 5 shows the percentage error of the SIF for fixed frequency $k_{\mathrm{T}}a = 0.05$ where SPM scheme is used. It is shown that the influence of the SQP-BE length l_{SQP} is not sensitive. Fig. 6 presents the percentage error of the SIF for two different frequencies at solution of the Q problem by the traction BIE and with SPM scheme. Here the shifted point is at the distance $l_i/8$ from the nodal point, where l_i is the BE length and at the distance $l_{QP}/16$ in the case of the crack-tip BE. In this case the obtained error curves at two different frequencies are very good.

Table 1 shows that the choice of the best intervals of the ratio l_{QP}/a where the solution of the problem W by the traction BIE and AM or SPM schemes is accurate and stable depends strongly on the frequency of the dynamic load. The values of the ratio l_{QP}/a giving an accurate and stable solution decrease with the increasing of the frequency.

The AM and SPM validation study shows in a strongly way that both numerical schemes are equivalent concerning the obtained accuracy and convergence results (Fig. 4). However, the AM can be used for the satisfaction of the (Hö)

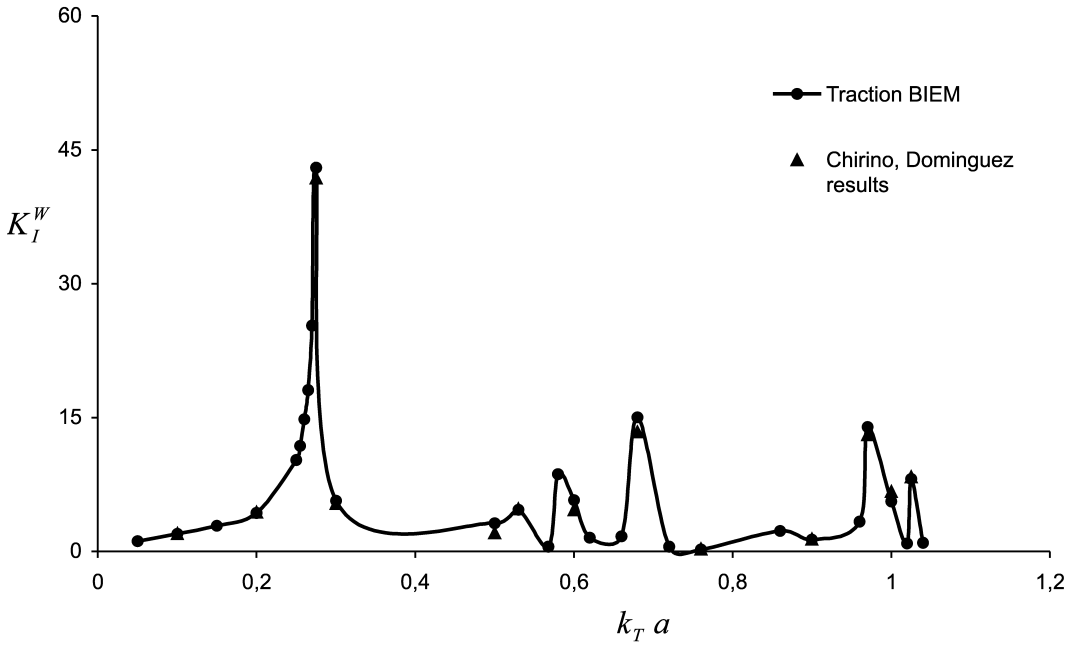

Fig. 3. Normalized SIF $K_{\mathrm{I}}^{\mathrm{W}}$ for centre cracked plate (problem W) under uniform time-harmonic traction obtained by traction BIEM and SPM numerical scheme.

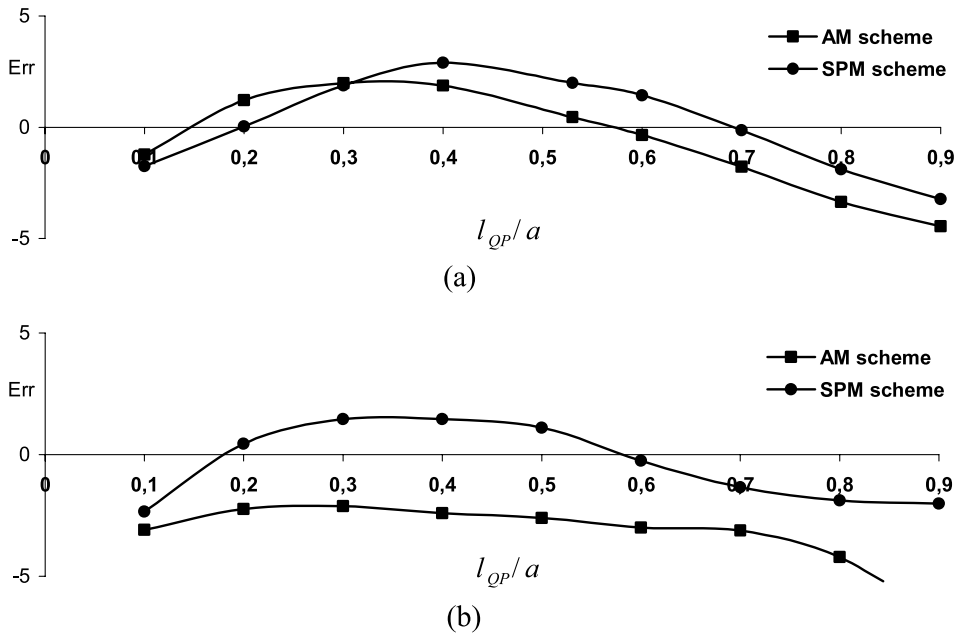

Fig. 4. Percentage error in SIF calculation obtained by the traction BIE for W problem at: (a) $k_{\mathrm{T}}a = 0.05$; (b) $k_{\mathrm{T}}a = 0.1$.

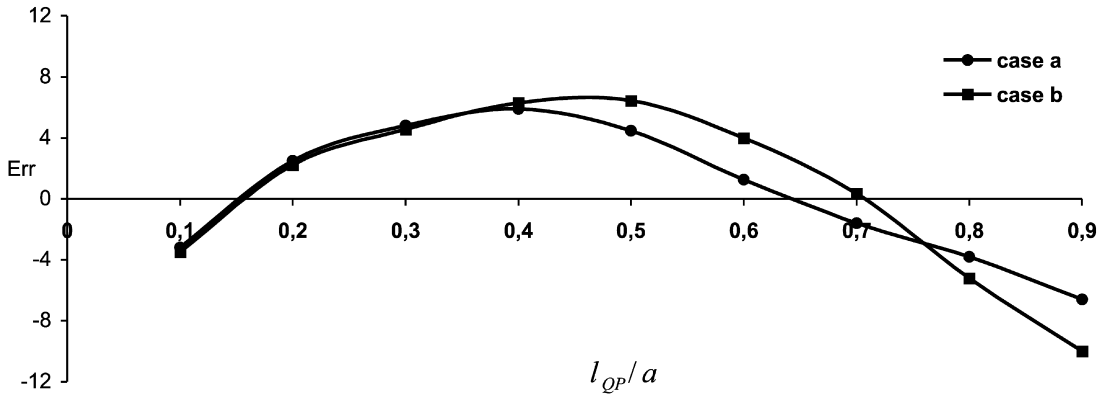

Fig. 5. Percentage error in SIF calculation at solution of the Q problem by the traction BIE at $k_{\mathrm{T}}a = 0.05$ using the SPM numerical scheme at: (a) $l_{\mathrm{SQP}} = 1.5$ mm; (b) $l_{\mathrm{SQP}} = 0.5$ mm.

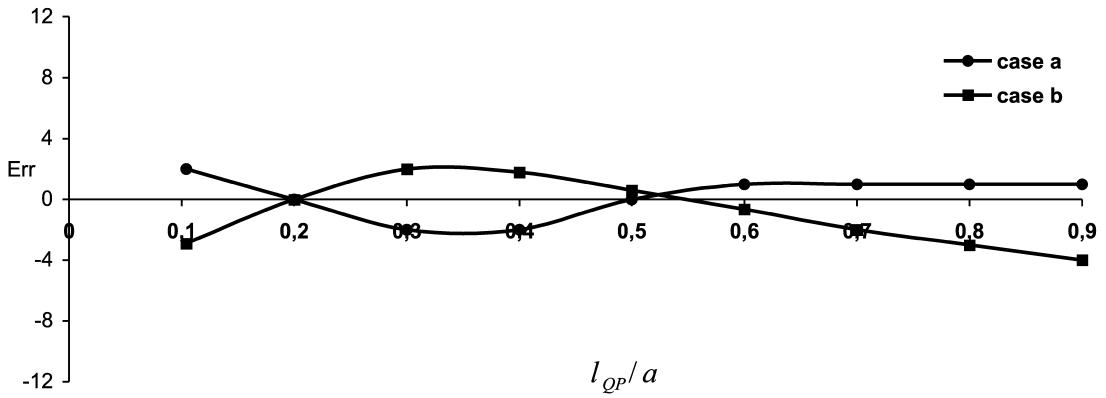

Fig. 6. Percentage error in SIF calculation at solution of the Q problem by the traction BIE using the SPM numerical scheme at: (a) $k_{\mathrm{T}}a = 0.05$; (b) $k_{\mathrm{T}}a = 0.98$.

Table 1
The intervals of l_{QP}/a where the solution of the problem W by the traction BIEM is accurate and stable

Frequency (s^{-1})	$\omega a/C_T$	SPM scheme	AM scheme
78,446.40	0.05	0.10–0.9	0.10–0.90
156,892.80	0.10	0.10–0.8	0.05–0.80
407,921.28	0.26	0.05–0.7	0.07–0.09
627,571.20	0.40	0.05–0.5	0.05–0.09
1,537,549.44	0.98	0.05–0.5	0.05–0.07

continuity only in the odd nodes, while the SPM can be used in all irregular points-odd nodes, corners and crack-tips.

3.2. Infinite cracked plane

Since under the analysis in Section 3.1, the SPM scheme is more simple in use and less cumbersome we show how it works for the well-known example of a single line crack in a complete plane under the incident P-wave (Fig. 7).

Let the crack has a length $2a = 10$ m and it lies on Ox axis on the interval $(-5, 5)$. The elastic constants are $\nu = 0.25$, $\lambda = \mu = 2.2165 \times 10^{10}$ N/m^2, $\rho = 2.4 \times 10^3$ kg/m^3. Let the frequencies are $\omega_l = [l(C_L \times 0.1)]/a$, $l = 1, \ldots, 7$. The number of BE on the crack is 5: 1st BE is LQP–BE; 2nd, 3rd, 4th are ordinary BE; 5th is RQP–BE, with length correspondingly $l_1 = 0.75$, $l_2 = 2.8$, $l_3 = 2.9$, $l_4 = 2.8$, $l_5 = 0.75$. The ξ coordinates of the shifted points are: $\xi = 0.75$ on 1st and 2nd BE; $\xi = -0.75$ on 4th and 5th BE.

The incident P-wave is defined with the potentials

$$\begin{cases} \Phi = \exp[-ik_L(x\cos\theta + y\sin\theta) - i\omega t] \\ \Psi = 0 \end{cases} \tag{14}$$

where θ is the direction of the plane wave.

It is used traction BIEM derived in Ref. [12]. Singular integrals are calculated analytically near field point on the symmetric intervals with a length in ξ coordinates equal 0.5, and numerically on the rest intervals. The program code is created using Mathematica system [27]. SIF is calculated for different values of θ and is normalized by its static value $\sigma = \mu k_T^2 \sqrt{\pi a}$.

In Fig. 8 are shown SIF modes I and II versus $k_L a$,

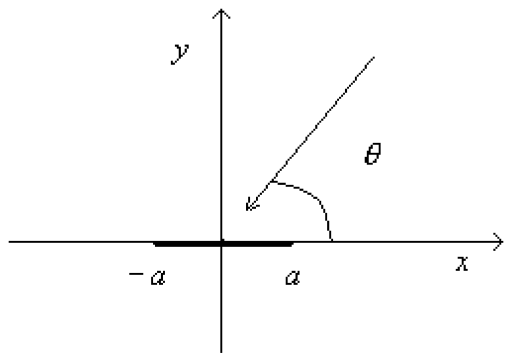

Fig. 7. Incident wave in a cracked plane.

calculated using traction formulae, where traction is calculated at the point with coordinates $(5.25, 0)$ (Appendix D). The comparison with the results of Chen and Sih [19] is very good. Note that the same test example is solved in Ref. [18] with a multidomain displacement BIEM where the BE mesh is not only on the crack but also at a distance to the crack tip equal to $15a$. The solution presented here with the traction BIEM and SPM scheme gives the same accuracy using 5 BE and the BE mesh is only on the crack.

4. Conclusions

The applicability of the hyper-singular traction BIEM for the solution of the dynamic time-harmonic problems of finite cracked bodies is studied. A centrally cracked plate under uniform time-harmonic tension is chosen as a model problem. The test example of a single crack in an infinite plane is also presented. It is shown by numerical results that the accuracy and the convergence of the hyper-singular traction BIEs for solution of the elastodynamic problems of a finite cracked bodies depends mainly on the type and the length of the special crack-tip elements, the frequency of the time-harmonic load and the smoothness requirements at all collocation points.

The disadvantages of the standard quadratic approximation concerning the smoothness at crack-tips, corners and odd nodes are discussed. Two new computational schemes as AM and SPM for overcoming of the described deficiencies of the continuous quadratic approximation are proposed and compared in order to obtain an accurate and stable solution.

The AM scheme based on the averaging of the tangential derivatives of displacements over the neighbouring boundary elements works well for all odd nodes. The SPM scheme based on the shifting of the collocation point keeps the continuous character of the parabolic approximation and works for odd nodes, corner points and crack-tip points. The SPM is easy to use and more simple than AM for numerical implementation in the already existing BIEM codes.

Some recommendations can be given based on the numerical study:

- The most crucial factor for the accuracy and the stable solution of dynamic fracture problems is the satisfaction of the smoothness condition in the odd boundary nodes when the standard parabolic approximation is used.
- The intervals of the ratio of the QP-BE length and the crack half-length where the solution of the traction BIE is accurate and stable in both schemes of the AM and SPM depend on the frequency. With increasing of the frequency the value of the ratio l_{QP}/a has to decrease in order to obtain a better accuracy.

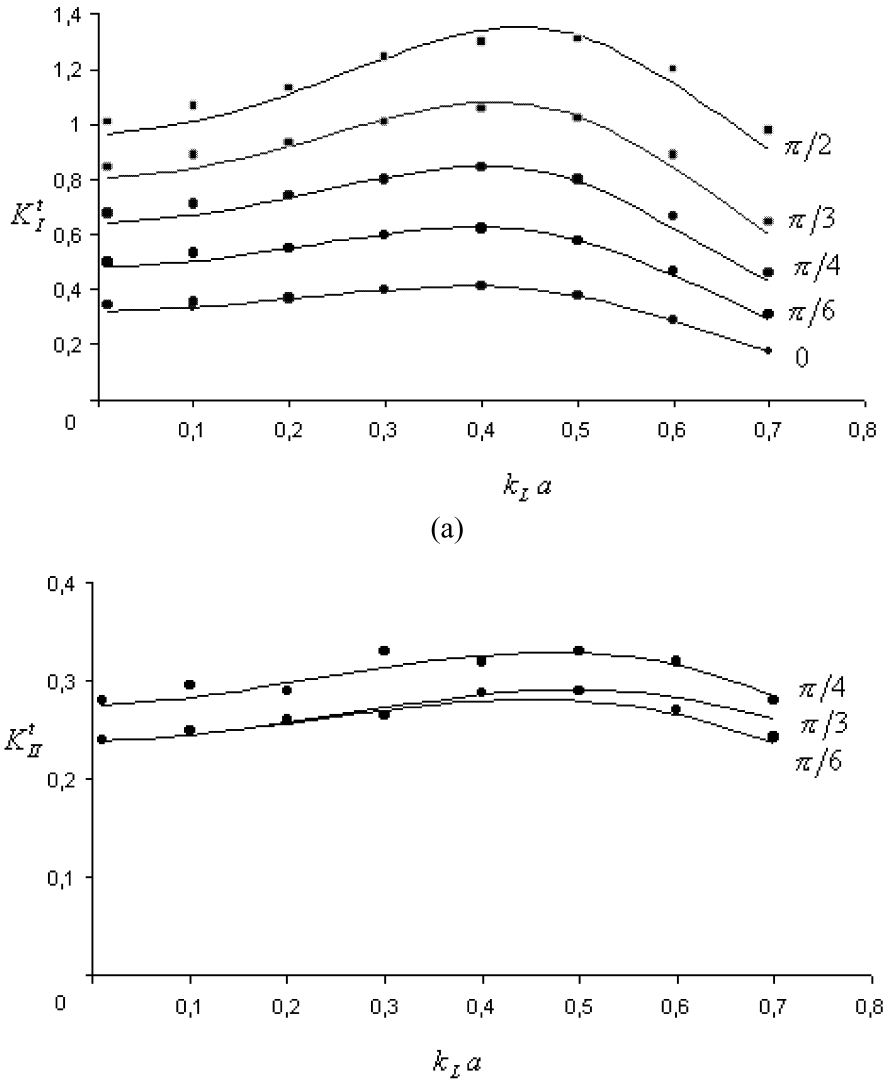

Fig. 8. Normalized SIF for a line crack in an infinite plane for incident P-wave by the traction BIEM using SPM numerical scheme and obtained by the traction formulae: (a) K_{I}^t; (b) K_{II}^t. (—) the present results; (●) the Chen and Sih [19] results.

The results obtained in this paper show that the hyper-singular traction BIEM together with the continuous parabolic type of approximation plus AM or SPM scheme can be used for solution of the dynamic fracture problems in finite multilayered solids with internal and interface cracks.

Acknowledgements

The authors acknowledge the support of the DFG under the grant number GR596/29-1.

Appendix A. Displacement and traction fundamental solutions

Function $U_{kj}^*(x, y, x_0, y_0, \omega)$ is the fundamental solution of system (1), $U_{kj,l}^*(x, y, x_0, y_0, \omega)$ are its derivatives and $P_{kj}^*(x, y, x_0, y_0, \omega)$ is the corresponding traction.

$$U_{kj}^*(x^p - x^q, y^p - y^q, \omega) = \frac{1}{2\pi\mu}[\psi\delta_{kj} - \chi r_{,k} r_{,j}]$$

$$\begin{aligned} P_{kj}^*(x^p - x^q, y^p - y^q, \omega) &= \frac{1}{2\pi}\left\{\left(\frac{\partial\psi}{\partial r} - \frac{\chi}{r}\right)\left(\delta_{kj}\frac{\partial r}{\partial n} + r_{,k} n_j\right) - 2\frac{\chi}{r}\left(r_{,j} n_k - 2r_{,k} r_{,j}\frac{\partial r}{\partial n}\right)\right\} \\ &\quad - \frac{1}{2\pi}\left\{2\frac{\partial\chi}{\partial r} r_{,k} r_{,j}\frac{\partial r}{\partial n} - \left(\frac{C_{\mathrm{L}}^2}{C_{\mathrm{T}}^2} - 2\right)\left(\frac{\partial\psi}{\partial r} - \frac{\partial\chi}{\partial r} - \frac{\chi}{r}\right) r_{,j} n_k\right\} \end{aligned}$$

$$\begin{aligned} U_{kj,l}^*(x^p - x^q, y^p - y^q, \omega) &= -\frac{1}{2\pi\mu}\left\{\frac{\partial\psi}{\partial r} r_{,l}\delta_{kj} - \frac{\partial\chi}{\partial r} r_{,l} r_{,k} r_{,j} - \chi[r_{,kl} r_{,j} + r_{,k} r_{,jl}]\right\} \end{aligned}$$

where

$$r=\sqrt{(x^p-x^q)^2+(y^p-y^q)^2},\quad r_{,x^q}=\frac{r_x}{r}=\frac{x^q-x^p}{r},$$

$$r_{,y^q}=\frac{r_y}{r}=\frac{y^q-y^p}{r}$$

(x^p,y^p) and (x^q,y^q) are the field point and the running point, respectively,

$$\frac{\partial r}{\partial n}=r_{,x^q}n_{x_0}+r_{,y^q}n_{y_0},\quad s=-\mathrm{i}\omega,\quad \chi=K_2\left(\frac{sr}{C_\mathrm{T}}\right)-\frac{C_\mathrm{T}^2}{C_\mathrm{L}^2}K_2\left(\frac{sr}{C_\mathrm{L}}\right)$$

$$\psi=\frac{1}{2}\left[K_2\left(\frac{sr}{C_\mathrm{T}}\right)-\frac{C_\mathrm{T}^2}{C_\mathrm{L}^2}K_2\left(\frac{sr}{C_\mathrm{L}}\right)+K_0\left(\frac{sr}{C_\mathrm{T}}\right)+\frac{C_\mathrm{T}^2}{C_\mathrm{L}^2}K_0\left(\frac{sr}{C_\mathrm{L}}\right)\right],$$

$K_m(z)$ are modified Bessel functions of the second kind [28], for $z=-\mathrm{i}\omega/C_{\mathrm{T,L}}$.

The asymptotic representations of the functions U^*_{kj}, $U^*_{kj,l}$ and P^*_{kj} for $r\to 0$ have the form [2]

$$(U^*_{kj})^{\mathrm{as}}\approx-\frac{1}{4\pi\mu}\left\{\left(1+\frac{C_\mathrm{T}^2}{C_\mathrm{L}^2}\right)\ln r\delta_{kj}-\left(1-\frac{C_\mathrm{T}^2}{C_\mathrm{L}^2}\right)r_{,k}r_{,j}\right\}$$

$$(U^*_{kj,l})^{\mathrm{as}}\approx-\frac{1}{4\pi\mu r}\left[\left(1+\frac{C_\mathrm{T}^2}{C_\mathrm{L}^2}\right)r_{,l}\delta_{kj}-\left(1-\frac{C_\mathrm{T}^2}{C_\mathrm{L}^2}\right)\times\left(r_{,j}\delta_{kl}+r_{,k}\delta_{jl}\right)+2\left(1-\frac{C_\mathrm{T}^2}{C_\mathrm{L}^2}\right)r_{,k}r_{,j}r_{,l}\right]$$

$$(P^*_{kj})^{\mathrm{as}}\approx-\frac{1}{2\pi r}\frac{C_\mathrm{T}^2}{C_\mathrm{L}^2}\left\{\left[\delta_{kj}-2\left(1-\frac{C_\mathrm{L}^2}{C_\mathrm{T}^2}\right)r_{,k}r_{,j}\right]\frac{\partial r}{\partial n}-[n_kr_{,j}-n_jr_{,k}]\right\}$$

Appendix B. Transformations from the global to intrinsic coordinates

For BE with a length l, nodes (x_1^q,y_1^q), (x_2^q,y_2^q), (x_3^q,y_3^q) and coordinates of the field point (x^p,y^p) transformations are as follows.

Ordinary BE:

$$\begin{vmatrix} r_x=r_{x_1}+\dfrac{\xi+1}{2}(r_{x_3}-r_{x_1})\\ r_y=r_{y_1}+\dfrac{\xi+1}{2}(r_{y_3}-r_{y_1})\end{vmatrix},\qquad \begin{vmatrix} r_{x_1}=x_1^q-x^p\\ r_{y_1}=y_1^q-y^p\end{vmatrix},$$

$$\begin{vmatrix} r_{x_3}=x_3^q-x^p\\ r_{y_3}=y_3^q-y^p\end{vmatrix},\qquad \begin{vmatrix} \dfrac{\mathrm{d}r_x}{\mathrm{d}\xi}=\dfrac{r_{x_3}-r_{x_1}}{2}\\ \dfrac{\mathrm{d}r_y}{\mathrm{d}\xi}=\dfrac{r_{y_3}-r_{y_1}}{2}\end{vmatrix},$$

$$J=\sqrt{\left(\frac{\mathrm{d}r_x}{\mathrm{d}\xi}\right)^2+\left(\frac{\mathrm{d}r_y}{\mathrm{d}\xi}\right)^2}=\frac{l}{2},\qquad \begin{vmatrix} n_x=\dfrac{\mathrm{d}r_y}{\mathrm{d}\xi}\dfrac{2}{l}\\ n_y=-\dfrac{\mathrm{d}r_x}{\mathrm{d}\xi}\dfrac{2}{l}\end{vmatrix}$$

Left QP-BE:

$$\begin{vmatrix} r_x=r_{x_1}+\left(\dfrac{\xi+1}{2}\right)^2(r_{x_3}-r_{x_1})\\ r_y=r_{y_1}+\left(\dfrac{\xi+1}{2}\right)^2(r_{y_3}-r_{y_1})\end{vmatrix},\qquad \begin{vmatrix} r_{x_1}=x_1^q-x^p\\ r_{y_1}=y_1^q-y^p\end{vmatrix},$$

$$\begin{vmatrix} r_{x_3}=x_3^q-x^p\\ r_{y_3}=y_3^q-y^p\end{vmatrix},\qquad \begin{vmatrix} \dfrac{\mathrm{d}r_x}{\mathrm{d}\xi}=(\xi+1)\dfrac{r_{x_3}-r_{x_1}}{2}\\ \dfrac{\mathrm{d}r_y}{\mathrm{d}\xi}=(\xi+1)\dfrac{r_{y_3}-r_{y_1}}{2}\end{vmatrix},$$

$$J=\sqrt{\left(\frac{\mathrm{d}r_x}{\mathrm{d}\xi}\right)^2+\left(\frac{\mathrm{d}r_y}{\mathrm{d}\xi}\right)^2}=(\xi+1)\frac{l}{2},$$

$$\begin{vmatrix} n_x=\dfrac{\mathrm{d}r_y}{\mathrm{d}\xi}\dfrac{2}{l(\xi+1)}\\ n_y=-\dfrac{\mathrm{d}r_x}{\mathrm{d}\xi}\dfrac{2}{l(\xi+1)}\end{vmatrix}$$

Right QP-BE:

$$\begin{vmatrix} r_x=r_{x_3}+\left(\dfrac{\xi-1}{2}\right)^2(r_{x_1}-r_{x_3})\\ r_y=r_{y_3}+\left(\dfrac{\xi-1}{2}\right)^2(r_{y_1}-r_{y_3})\end{vmatrix},\qquad \begin{vmatrix} r_{x_1}=x_1^q-x^p\\ r_{y_1}=y_1^q-y^p\end{vmatrix},$$

$$\begin{vmatrix} r_{x_3}=x_3^q-x^p\\ r_{y_3}=y_3^q-y^p\end{vmatrix},\qquad \begin{vmatrix} \dfrac{\mathrm{d}r_x}{\mathrm{d}\xi}=(\xi-1)\dfrac{r_{x_1}-r_{x_3}}{2}\\ \dfrac{\mathrm{d}r_y}{\mathrm{d}\xi}=(\xi-1)\dfrac{r_{y_1}-r_{y_3}}{2}\end{vmatrix},$$

$$J=\sqrt{\left(\frac{\mathrm{d}r_x}{\mathrm{d}\xi}\right)^2+\left(\frac{\mathrm{d}r_y}{\mathrm{d}\xi}\right)^2}=(1-\xi)\frac{l}{2},$$

$$\begin{vmatrix} n_x=\dfrac{\mathrm{d}r_y}{\mathrm{d}\xi}\dfrac{2}{l(1-\xi)}\\ n_y=-\dfrac{\mathrm{d}r_x}{\mathrm{d}\xi}\dfrac{2}{l(1-\xi)}\end{vmatrix}$$

Appendix C. Shape functions

Quadratic shape functions and their derivatives:

$$N_1=\frac{\xi(\xi-1)}{2},\qquad N_2=1-\xi^2,\qquad N_3=\frac{\xi(1+\xi)}{2};$$

$$N_1'=\xi-\tfrac{1}{2},\qquad N_2'=-2\xi,\qquad N_3'=\xi+\tfrac{1}{2},$$

$$\begin{pmatrix}N_1'\\N_2'\\N_3'\end{pmatrix}=\begin{pmatrix}-1.5&-0.5&0.5\\2&0&-2\\-0.5&0.5&1.5\end{pmatrix}\begin{pmatrix}N_1\\N_2\\N_3\end{pmatrix}$$

Appendix C1. Special singular crack-tip shape functions

Right SQP-BE defined in $[-1, 1)$ and $N_3^{*r} \approx O(1/(1-\xi))$ for $\xi \to 1$

$$\begin{pmatrix} N_1^{*r} \\ N_2^{*r} \\ N_3^{*r} \end{pmatrix} = \frac{2}{N_2 + 2N_1} \begin{pmatrix} N_1 \\ N_2 \\ N_3 \end{pmatrix}$$

Left SQP-BE defined in $[-1, 1)$ and $N_1^{*l} \approx O(1/(1+\xi))$ for $\xi \to -1$

$$\begin{pmatrix} N_1^{*l} \\ N_2^{*l} \\ N_3^{*l} \end{pmatrix} = \frac{2}{N_2 + 2N_3} \begin{pmatrix} N_1 \\ N_2 \\ N_3 \end{pmatrix}$$

Appendix D. SIF two-point displacement and traction formulae

SIF formulae are described in Ref. [29].

Displacement formulae for the problem (W):

$$K_{\mathrm{I}}^{\mathrm{W}} = \frac{\mu}{4(1-\nu)} \sqrt{\frac{2\pi}{l_{\mathrm{QP}}}} (4\Delta u_y^2 - \Delta u_y^1),$$

$$K_{\mathrm{II}}^{\mathrm{W}} = \frac{\mu}{4(1-\nu)} \sqrt{\frac{2\pi}{l_{\mathrm{QP}}}} (4\Delta u_x^2 - \Delta u_x^1)$$

Displacement formulae for the problem (Q):

$$K_{\mathrm{I}}^{\mathrm{Q}} = \frac{\mu}{2(1-\nu)} \sqrt{\frac{2\pi}{l_{\mathrm{QP}}}} (4u_y^2 - u_y^1),$$

$$K_{\mathrm{I}}^{\mathrm{Q}} = \frac{\mu}{2(1-\nu)} \sqrt{\frac{2\pi}{l_{\mathrm{QP}}}} (4u_x^2 - u_x^1)$$

Traction formulae:

$$K_{\mathrm{I}}^{t} = \sqrt{2\pi l_0} p_y(z_0), \qquad K_{\mathrm{II}}^{t} = \sqrt{2\pi l_0} p_x(z_0)$$

Here u_j^2, u_j^1 are the components of displacement at the second and first node of the QP-BE, $p_j(z_0)$ is the value of the traction at the point z_0 and $l_0 = |z_0 - a|$.

References

[1] Cruse TA. Two-dimensional BIE fracture mechanics analysis. Appl Math Model 1978;2:287–93.

[2] Sladek J, Sladek V. Transient elastodynamic three-dimensional problems in cracked bodies. Appl Math Model 1984;8:2–10.

[3] Sladek J, Sladek V. A BIEM for dynamic crack problems. Engng Fract Mech 1987;27:269–77.

[4] Chirino Fr, Gallego R, Dominguez J. A comparative study of three-boundary element approaches to transient dynamic crack problems. Engng Anal BE 1994;13:11–19.

[5] Snyder MD, Cruse TA. BIE analysis of cracked anisotropy plates. Int J Fract 1975;11:315–28.

[6] Balas J, Sladek J, Sladek V. Stress analysis by boundary element methods. Amsterdam: Elsevier; 1989.

[7] Budreck DE, Achenbach JD. Scattering from three-dimensional planar cracks by the BIEM. ASME J Appl Mech 1988;55:405–12.

[8] Hirose S, Achenbach JD. Application of BEM to transient analysis of a 3-D crack. In: Tanaka M, Cruse TA, editors. BEM in applied mechanics. Oxford: Pergamon Press; 1988. p. 255–64.

[9] Hirose S, Achenbach JD. Acoustic emission and near-tip elastodynamic fields of a growing penny-shaped crack. Engng Fract Mech 1991;39:21–36.

[10] Dineva P, Gross D, Rangelov Ts. Ultrasonic wave scattering by a line crack in a solder joint. Res Nondestruct Eval 1999;11:117–35.

[11] Zhang Ch, Achenbach JD. A new boundary integral equation formulation for elastodynamic and elastostatic crack analysis. ASME J Appl Mech 1989;56:284–90.

[12] Zhang Ch, Gross D. On wave propagation in elastic solids with cracks. Southampton: Computation Mechanics Publications; 1998.

[13] Chirino F, Abascal R. Dynamic and static analysis of cracks using the hypersingular formulation of the boundary element method. Int J Numer Meth Engng 1998;43:365–88.

[14] Fidelinski P, Aliabadi M, Rooke D. The dual boundary element method in dynamic fracture mechanics. Engng Anal BE 1993;12:203–10.

[15] Chen J, Hong H-K. Review of dual boundary element methods with emphasis on hypersingular integrals and divergent series. Appl Mech Rev 1999;52:17–33.

[16] Portela A, Aliabadi MH. The dual BEM: effective implementation for crack problems. Int J Numer Meth Engng 1992;33:1269–87.

[17] Zhang Ch. A novel derivation of non-hypersingular time-domain BIEs for transient elastodynamic crack analysis. Int J Solid Struct 1991;28:267–81.

[18] Chirino Fr, Dominguez J. Dynamic analysis of cracks using BEM. Engng Fract Mech 1989;34:1051–61.

[19] Chen EP, Sih GC. Scattering waves about stationary and moving cracks. In: Sih GC, editor. Mechanics of fracture: elastodynamic crack problems. Leyden: Noordhoff; 1977. p. 119–212.

[20] Krishnasamy G, Schmerr LW, Rudolphi TJ, Rizzo FJ. Hypersingular boundary integral equations: some applications in acoustic and elastic wave scattering. Trans ASME 1990;57:404–14.

[21] Martin PA, Rizzo FJ. On boundary integral equations for crack problems. Proc R Soc Lond A 1989;421:341–55.

[22] Sih GC, Loeber JE. Wave propagation in an elastic solid with a line of discontinuity or finite crack. Quart J Appl Math 1969;27:193–213.

[23] Blandford GE, Ingrafea AR, Ligget JA. Two-dimensional stress intensity factor computations using the boundary element method. Int J Numer Meth Engng 1981;17:387–404.

[24] Gelfand I, Shilov G, Generalized functions, vol. 1. New York: Academic Press; 1964.

[25] Dineva P, Gross D, Rangelov Ts. Dynamic behaviour of a cracked solder joint. J Sound Vib 2002;256:81–102.

[26] Dineva P, Gross D, Rangelov Ts. Dynamic behaviour of a bi-material rectangular plate with interface cracks under uniform time-harmonic tension. Engng Fract Mech 2002;69:1193–218.

[27] Wolfram S. A system for doing Mathematics by computer, 3rd ed. Cambridge: Cambridge University Press; 2000.

[28] Bateman H, Erdelyi A. Higher transcendental functions. New York: McGraw-Hill; 1953.

[29] Aliabadi MH, Rooke DP. Numerical fracture mechanics. Southampton: Computation Mechanics Publications; 1991.